J Mol Model (2013) 19:1459–1471
DOI 10.1007/s00894-012-1707-6

ORIGINAL PAPER

Microsolvation and hydration enthalpies of $CaC_2O_4(H_2O)_n$ (n=0-16) and $C_2O_4^{2-}(H_2O)_n$ (n=0-14): an *ab initio* study

Victor M. Rosas-García · Isabel del Carmen Sáenz-Tavera · Verónica Janeth Rodríguez-Herrera · Benjamín Raymundo Garza-Campos

Received: 15 October 2012 / Accepted: 20 November 2012 / Published online: 12 December 2012

Abstract We studied hydrated calcium oxalate and its ions at the restricted Hartree–Fock RHF/6-31G* level of theory. Performing a configurational search seems to improve the fit of the HF/6-31G* level to experimental data. The first solvation shell of calcium oxalate contains 13 water molecules, while the first solvation shell of oxalate ion is formed by 14 water molecules. The first solvation shell of Ca(II) is formed by six water molecules, while the second shell contains five. At 298.15 K, we estimate the asymptotic limits (infinite dilution) of the total standard enthalpies of hydration for Ca(II), oxalate ion and calcium oxalate as −480.78, –302.78 and –312.73 kcal mol^{-1}, resp. The dissociation of hydrated calcium oxalate is an endothermic process with an asymptotic limit of +470.84 kcal mol^{-1}.

Keywords *Ab initio* · Calcium ion · Calcium oxalate · Hydration enthalpy · Hydration shell · Oxalate ion

Introduction

Ionic and molecular hydration is an area of very active experimental and theoretical investigation [1–7]. Knowledge about the number of solvent molecules necessary to stabilize a solute and the solvent-solvent interactions is required for understanding the dissolution process, as well as the solvation-desolvation changes involved in the interaction with biomolecules.

Calcium oxalate is of interest due to its dual participation in pathologies such as kidney stones, either as the main constituent of the stones in the form of calcium oxalate monohydrate (COM), or as the beneficial—although less stable—calcium oxalate dihydrate (COD) which functions as a protective agent against kidney stone formation [8]. Despite its participation in biochemically and clinically interesting processes, studies of calcium oxalate hydration remain scarce.

There is great interest in understanding calcium solvation because, among other things, it is the most abundant cation in the human body [9, 10] and fulfills several roles in living systems, e.g., in metabolism control [11], muscle contraction [11, 12], clotting of blood [11, 12], cell division [12], transmission of nerve impulses [11, 13] and in building bone structure [11, 14]. At a molecular level, calcium helps to initiate events as basic as cell motility, contraction, secretion, and division [13, 15]. Calcium ion also binds to many proteins, such as calmodulin and annexins, and enables them to function [15, 16]. The binding behavior of calcium ion to carboxylate groups is similar in both small molecules and protein structures [14].

Hydration of Ca(II) has been studied experimentally by X-ray [9], blackbody infrared radiative dissociation [17], mathematical calculations from experimental gas-phase data [18] and measurements of colligative properties of water solutions of calcium salts [10]. While computationally, researchers have resorted to Car-Parrinello molecular dynamics [19, 20], classical MD, quantum mechanics/molecular mechanics (QM/MM) MD [16, 21–28], Hartree–Fock (HF) and density functional theory (DFT) simulations [14, 23, 25, 29–35] and ab initio effective pair potentials [36].

Other investigators combined experimental and theoretical methods in order to determine the coordination number and geometric and energetic values for hydrated Ca(II). They have used molecular dynamics and X-ray scattering [37] or extended X-ray absorption fine-structure spectroscopy (EXAFS) and large-angle X-ray scattering (LAXS) [21]. Megyes et al. [29] used X-ray diffraction and ab initio

V. M. Rosas-García (✉) · I. del Carmen Sáenz-Tavera · V. J. Rodríguez-Herrera · B. R. Garza-Campos
Facultad de Ciencias Químicas, Universidad Autónoma de Nuevo León (UANL), Ave. Pedro de Alba S/N, Ciudad Universitaria, San Nicolás de los Garza, N. L., Mexico 66451
e-mail: rosas.victor@gmail.com

calculations at HF/MP2 and B3LYP levels. Peschke et al. [30, 38] used determinations of equilibrium in gas phase and ab initio calculations at DFT B3LYP/6-311+G(d, p) level and Bush et al. [31, 32] used infrared spectroscopy combined with ab initio methods. In all cases, the experimental results matched the theoretical results [21, 29–32, 37], but there is still disagreement among the reported results, with the solvation shell of Ca(II) being reported as formed by 6–9 molecules of water (see Table 1).

Regarding oxalate solvation, Wang et al. [39] in 2001, studied oxalate ion aggregates in the gas phase by X-ray photoemission spectroscopy and later, in 2003, the same authors reproduced their experimental results by theoretical computation with density functional theory using the B3LYP functional and solvation by explicit water molecules [40]. With the same model but by molecular dynamics at RHF/6-31G* level, Gao and Liu [41] found similar results. We did not find reports about calcium oxalate hydration.

In this work, we examine the solvation shells and energetics of hydrated calcium oxalate and its ions using ab initio methods and an explicit solvent model. As Marcus pointed out [42], no consensus exists about the best

Table 1 Number of water molecules and Ca-O distance/Å in the first shell of hydrated Ca(II)

Number of water molecules	Ca-O distance/Å	Method		Reference
		Experimental	Computational	
6		Gas phase equilibrium determination	B3LYP/6-311+G(d, p)	[30]
6		IR laser action spectroscopy	B3LYP/LACVP++**	[31]
6	2.39		CPMD	[20]
6	2.42		B3LYP/6-311+G(d,p)	[33]
6	2.51		CPMD	[19]
6	2.58		RHF/6-31G*	This work
7		Blackbody IR radiative dissociation		[17]
7	2.50		QM/MM	[34]
7.1	2.50		MD	[23]
7.2	2.437	XAFS, EXAFS, XANES		[9]
7.2–7.7	2.42–2.46		MD	[16]
7.5	2.38		MD	[26]
7.6	2.46		QM/MM MD HF	[23]
7.7	2.48		MD	[27]
7.9	2.48		QM/MM MD HF	[25]
8		IR laser action spectroscopy	B3LYP/6-311++G(d, p)	[32]
8	2.48	X-ray diffraction	HF, MP2 and B3LYP/6-311+G**	[21]
8	2.46	EXAFS, LAXS	MD	[21]
9	2.39	X-ray scattering	MD	[37]
8 (between 20 °C and 30 °C)		Colligative properties		[10]
8		From experimental gas-phase data		[18]
8	2.48		B3LYP/6-311+G(2d,2p)	[35]
8	2.52		RHF/6-31G* for O and H, HUZSP for Ca, MP2	[14]
8	2.41		MD	[27]
8	2.51		MD	[24]
8			MD	[59]
8.0	2.48		QM/MM MD DFT	[25]
8.1	2.51		QM/MM MD DFT	[23]
8.3			MD	[22]
8.6			Ab initio effective pair potential	[36]
9.2			QM/MD	[22]

quantum mechanical level to model ion-water interactions. We reasoned that the performance of a relatively low level of theory (HF/6-31G*) could be improved by doing a configurational search to get closer to the global minimum enabling us to study larger species with limited computer equipment. HF/6-31G* has the advantage of being generally applicable to many systems. In addition, popular DFT functionals such as B3LYP, describe poorly hydrogen bonding [43], or are dependent on the directionality of the H-bond [44]. Other functionals recommended for H-bonding have a larger computational requirement than HF/6-31G*.

Methods

Software employed

Molecular structures were built using Ghemical [45]. Semiempirical molecular dynamics and preoptimizations employed the PM6 Hamiltonian implemented in MOPAC2009 [46]. Optimizations at the RHF/6-31G* level of theory used GAMESS-US [47] and ORCA v.2.9 [48]. Initial configurations for the MonteCarlo-like procedure were generated with PACKMOL [49]. Atom-atom distances were determined using Jmol [50]. Images were produced using Jmol and ray-traced by POV-Ray

Table 2 Optimized geometric parameters for $C_2O_4^{2-}(H_2O)_n$ and $CaC_2O_4(H_2O)_n$ using the RHF/6-31G* level of theory. O-C-C-O dihedrals are *gauche* angles

Number of water molecules	0	1	6	12[a]	14	16
$C_2O_4^{2-}(H_2O)_n$						
C-C bond length/Å	1.55	1.55	1.54	1.53(1.54)	1.53	n.d.
C-O bond length/Å	1.25	1.24	1.24	1.24	1.23	n.d.
		1.24	1.24	1.24	1.24	
		1.25	1.24	1.24	1.24	
		1.25	1.25	1.25(1.27)	1.25	
O-C-O bond angle/º	126.3	125.5	126.3	125.4	126.1	n.d.
		127.5	126.6	127.4(126.4)	127.1	
O-C-C bond angle/º	116.8	116.2	116.6	115.9	116.3	n.d.
		116.3	116.8	116.7	116.6	
		117.2	116.8	117.1	116.9	
		117.2	116.9	117.5(116.6)	117.0	
O-C-C-O dihedral angles/º	90.0 90.0	89.9 90.0	70.0	78.3	78.3 80.0	n.d.
			71.1	79.9		
$CaC_2O_4(H_2O)_n$						
C-C bond length/Å	1.59	1.58	1.54	1.53	1.56	1.54
C-O bond length/Å	1.19	1.19	1.20	1.21	1.22	1.21
	1.19	1.19	1.22	1.21	1.22	1.22
	1.30	1.30	1.28	1.27	1.26	1.27
	1.30	1.30	1.29	1.27	1.26	1.27
Ca-$O_{oxalate}$ bond distance/Å	2.15	2.17	2.37	2.41	2.39	2.44
	2.15	2.20	2.42	2.45	2.43	2.47
	4.13	4.16	3.93	4.10	4.17	4.11
	4.13	4.16	4.27	4.28	4.32	4.40
Ca-C distance/Å	2.97	3.00	3.02	3.11	3.11	3.12
	2.97	3.01	3.14	3.17	3.16	3.22
O-C-O bond angle/º	125.8	125.6	125.5	126.4	125.7	126.3
	125.8	126.3	128.0	126.9	127.1	127.0
O-C-C bond angle/º	114.8	114.2	109.5	111.5	113.8	112.9
	114.8	114.4	113.3	111.8	115.5	113.5
	119.4	119.3	120.7	121.4	118.7	120.1
	119.4	120.2	122.4	121.6	118.9	120.1
O-C-C-O dihedral angle/º	−0.1	−18.2	59.2	56.5	14.5	47.7
	−0.1	−17.0	68.2	64.7	15.4	52.1

[a] Values in parentheses are DFT results from ref. [41] for the more stable isomer

Table 3 Comparison of average Ca-O distances, in Å, for the first hydration shell in $Ca^{2+}(H_2O)n$, n=0-9

n	RHF/6-31G*[a]	MP2/6-311+G**[b]	Exp.
1	2.19	2.28	
2	2.23	2.31	
3	2.27	2.33	
4	2.33	2.35	
5	2.33	2.37	
6	2.40	2.40	
7	2.38	2.46	
8	2.38	2.48	2.48[c]
			2.43–2.46[d]

[a] This work, RHF/6-31G*. [b] MP2/6-311+G** from ref. [29]. [c] Ref. [30], DFT B3LYP. [d] Ref. [29] by X-ray diffraction, and ref [21], from EXAFS and LAXS

[51]. Cropping and color-to-grayscale transformation of the ray-traced images used GIMP v.2.6.7 [52].

Cluster structure optimization

We employed two general procedures, one based on molecular dynamics and the other on a MonteCarlo-like configurational search. Both methods involved building the molecular structure using Ghemical and submit to geometric optimization using the semiempirical Hamiltonian PM6 [53]. After this the methods diverged. The molecular dynamics search consisted of (a) taking the optimum semiempirical structure obtained, load it back into Ghemical and add one water molecule, (b) find the global minimum of the new structure searching by semiempirical molecular dynamics, (c) select the lowest energy structure and repeat the procedure from step (a) up to the total number of water molecules considered for each species. Each molecular dynamics run produced 1000 configurations using the dynamic reaction coordinate (DRC) facility present in MOPAC2009 and optimized the structures employing the PM6 Hamiltonian. The resulting minima were visualized to discard isomerized structures. The molecular dynamics runs were repeated until no new minima were obtained, which required a total of 25,000 structures for each cluster.

The Montecarlo-like procedure involved using PACKMOL to generate 50–100 initial configurations of water molecules around the calcium oxalate (a different random seed was used in each case).

The resulting configurations (either from PM6 DRC or from PACKMOL) were then optimized at the RHF/6-31G* level of theory and their vibrational frequencies calculated to characterize the stationary points obtained. All the structures we kept were true minima with only real frequencies. The global minima obtained (three structures) were also optimized and their vibrational frequencies calculated at the RI-MP2/def2-SVP level of theory

Determination of hydration shell structure

For each minimum obtained at the ab initio level, we determined the radial distribution function (RDF) of the water molecules using the oxygen (O_w) as a reference point for each water molecule. The RDF for Ca(II) was based on Ca-O_w distances; for oxalate ion and calcium oxalate, we calculated M-O_w distances, where M is the geometric centroid of the molecule.

The RDF, $g(r)$, is defined in Eq. (1) [54].

$$g(r) = \frac{n(r)/\Delta V}{N/V}, \tag{1}$$

where r is the distance between the central point (calcium ion or M) and an O_w atom, $n(r)$ is the number of O_w atoms included in the range between $r - \Delta r/2$ and $r + \Delta r/2$, ΔV is the volume of the spherical shell, N is the total number of O_w atoms and N/V is the number density of O_w atoms. We calculated $g(r)$ values every 0.4 Å and the thickness of each hydration shell was estimated as twice the radius of water [42, 55]. For each RDF we computed the running coordination number according to the formula given by Babu and Lim (Eq. 2) [3]:

$$n = 4\pi\rho \int_0^R g(r) r^2 dr. \tag{2}$$

Energy calculations and corrections

All the Hartree–Fock energies were computed at 298.15 K and corrected for zero-point energy (ZPE). Enthalpy values were calculated by adding the thermal corrections reported in the thermochemical analysis section to the ZPE-corrected total energy [56, 57].

Total ($\Delta_{hyd}H°$) and differential (succesive) ($\Delta_{diff}H°$) standard hydration enthalpies were calculated by Eqs. (3) and (4) respectively, for the processes shown in Scheme I,

$$\Delta_{diff}H^\circ = H^\circ X(H_2O)_n - \left(H^\circ X(H_2O)_{n-1} + H^\circ H_2O\right) \tag{3}$$

$$\Delta_{hyd}H^\circ = H^\circ X(H_2O)_n - (H^\circ X + nH^\circ H_2O). \tag{4}$$

Scheme I

$$X(H_2O)_{n-1} + H_2O \rightleftarrows X(H_2O)_n X + nH_2O \rightleftarrows X(H_2O)_n,$$

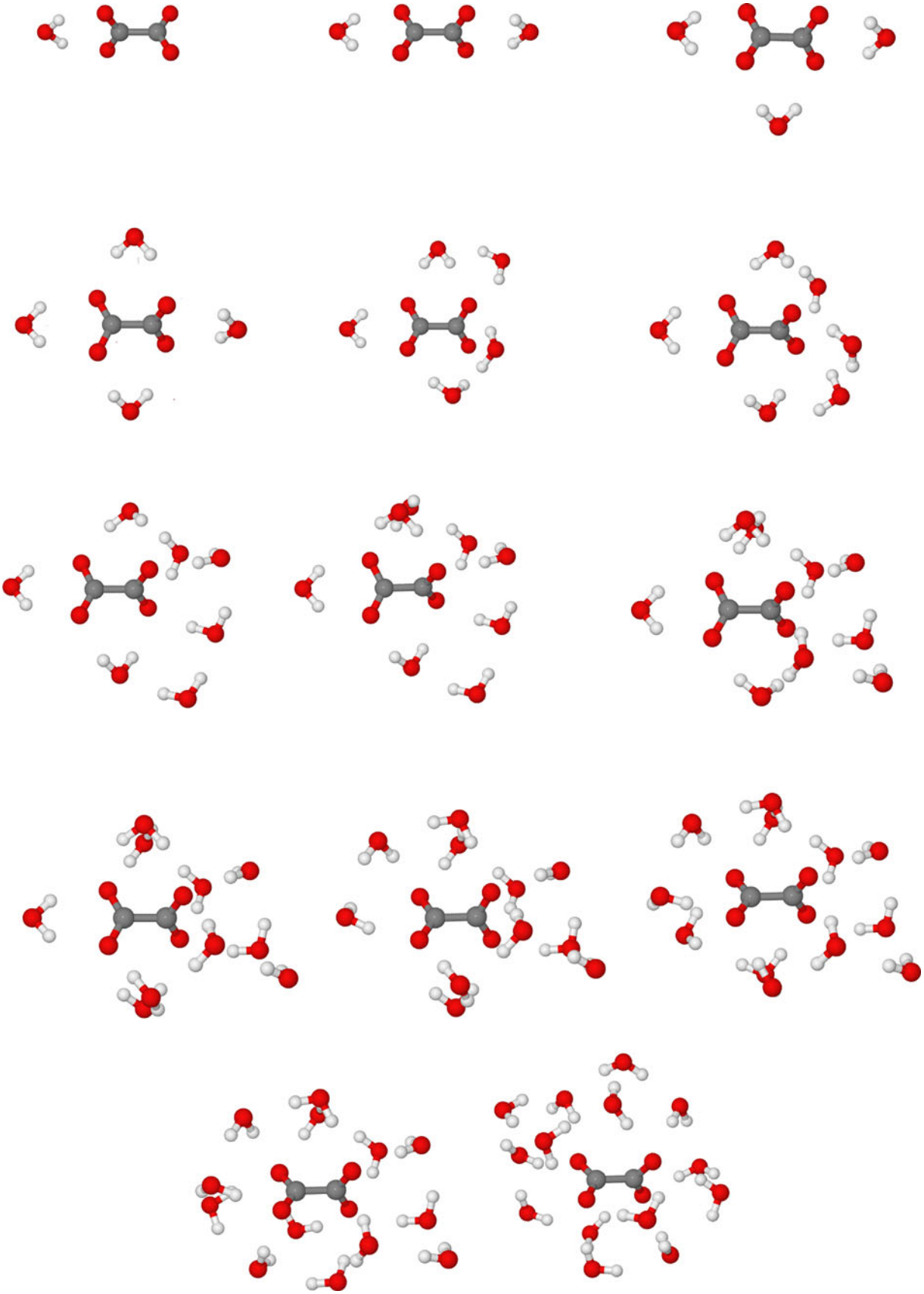

Fig. 1 Optimized geometries for $C_2O_4^{2-}(H_2O)_n$ using RHF/6-31G* level of theory, n=0-14

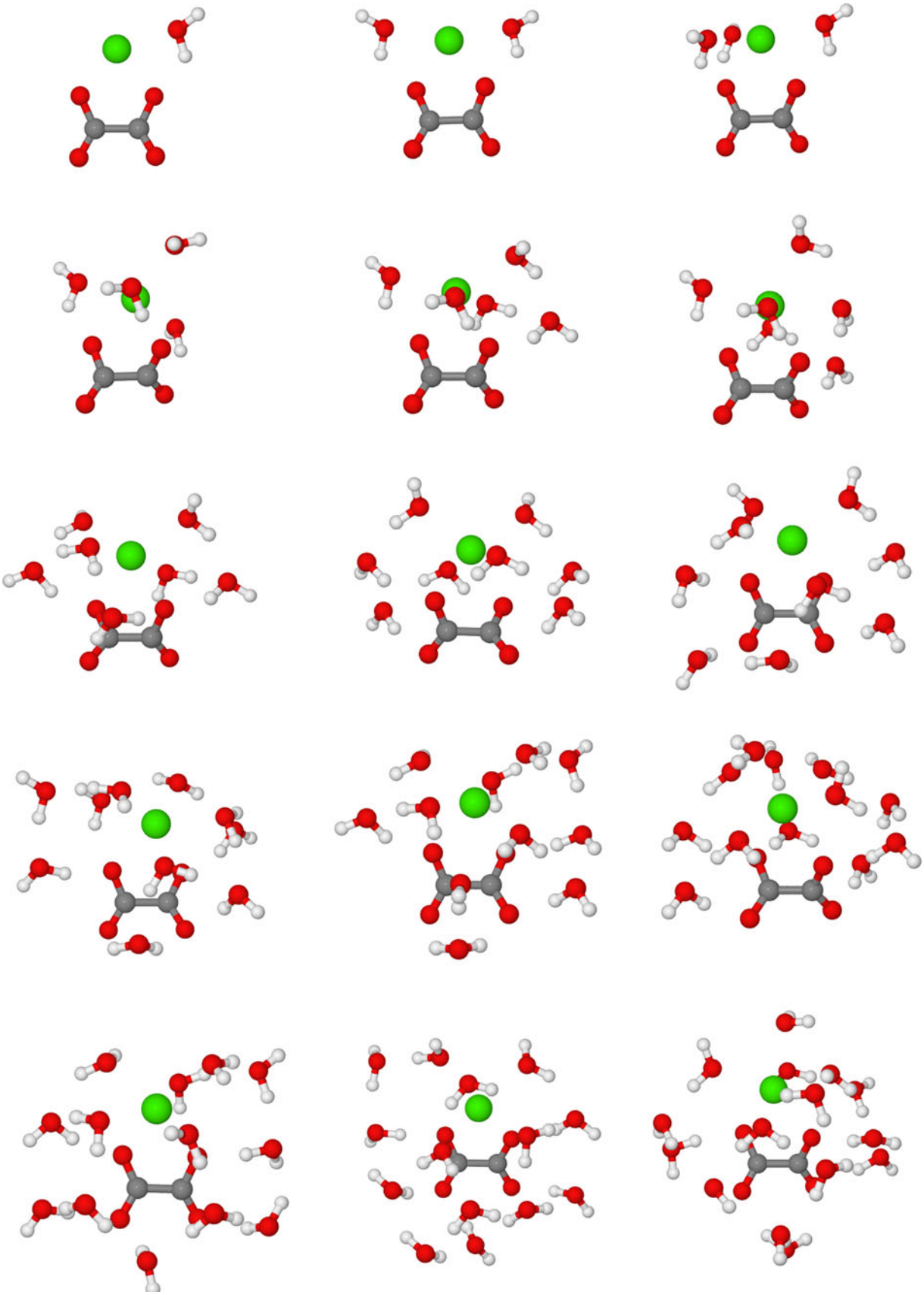

Fig. 2 Optimized geometries for $CaC_2O_4(H_2O)_n$ using RHF/6-31G* level of theory, n=0-16

where X=Ca^{2+}, $C_2O_4{}^{2-}$ and CaC_2O_4, n=0-14 for calcium ion, 0–14 for oxalate ion, and 0–16 for calcium oxalate.

The step-wise binding electronic energy ($\Delta_{step}E$) was calculated using Eq. (5).

$$\Delta_{step}E = E\,CaC_2O_4(H_2O)_n - \left(E\,C_2O_4{}^{2-}(H_2O)_{n-1} + E\,H_2O\right). \quad (5)$$

For the process shown in Scheme II,

Scheme II

$$CaC_2O_4(H_2O)_n \rightleftarrows Ca^{2+}(H_2O)_m + C_2O_4{}^{2-}(H_2O)_{n-m}$$
$$where \quad \left\{ \begin{array}{ll} n \le 9; & m = n \\ n > 9; & m = 9 \end{array} \right\},$$

where n=1-16. The choice of values for m is based on Woon and Dunning [58], who have shown that water preferentially solvates the cation over the anion when adding water molecules, so the first nine water molecules were used to solvate the Ca(II). Dissociation enthalpies ($\Delta_{diss}H°$) were calculated by Eq. (6),

$$\Delta_{diss}H^\circ = H^\circ{}_{Ca^{2+b}(H_2O)_m} + H^\circ{}_{C_2o_4^{2-b}(H_2O)_{n-m}} - H^\circ{}_{CaC_2O_4(H_2O)_n} \quad (6)$$

Results and discussion

Structures of solvated species and solvation shells

In calcium oxalate, the C-C bond starts abnormally long in the gas phase (1.59 Å) and this monotonically approaches a more common length, 1.55 Å, upon addition of water molecules. We attribute the stretched bond with no water molecules to coulombic repulsion of the negative charges on the oxygens. C-O bond distances are consistently longer on the oxygens closer to the calcium ion, an effect we attribute to

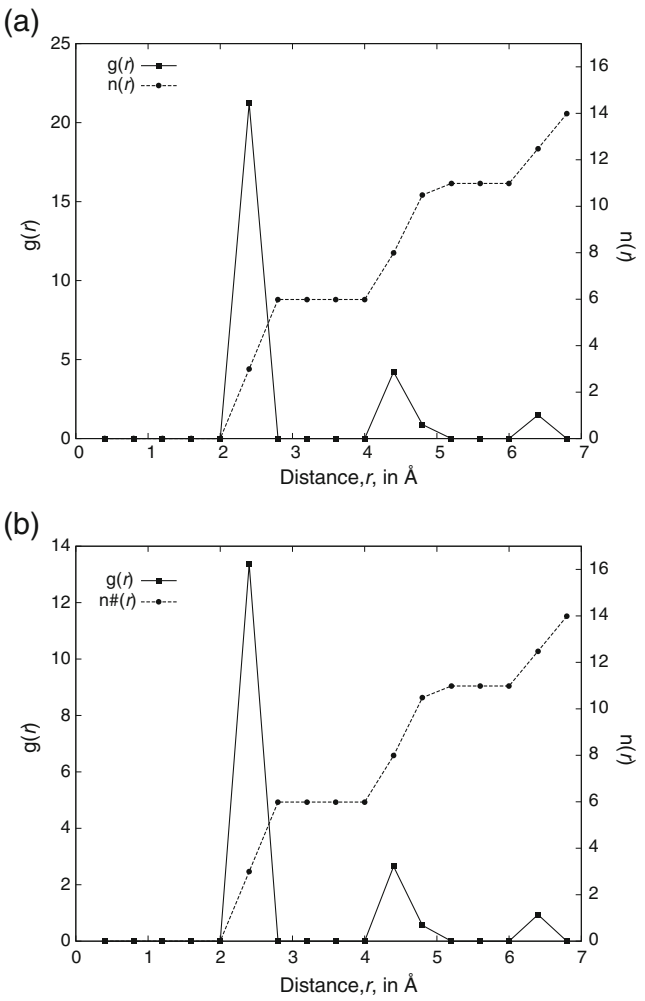

Fig. 3 Radial distribution function and running coordination number for $Ca^{2+}(H_2O)_{14}$ at **a** HF/6-31G* level of theory, and **b** RI-MP2/def2-SVP level of theory

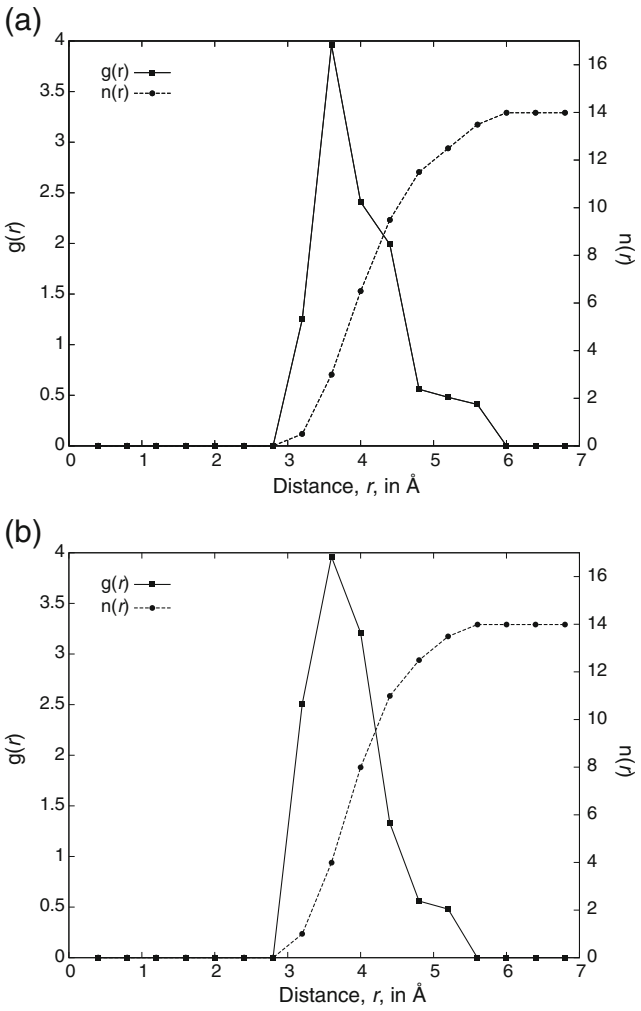

Fig. 4 Radial distribution function and running coordination number for $C_2O_4{}^{2-}(H_2O)_{14}$ at **a** HF/6-31G* level of theory, and **b** RI-MP2/def2-SVP level of theory

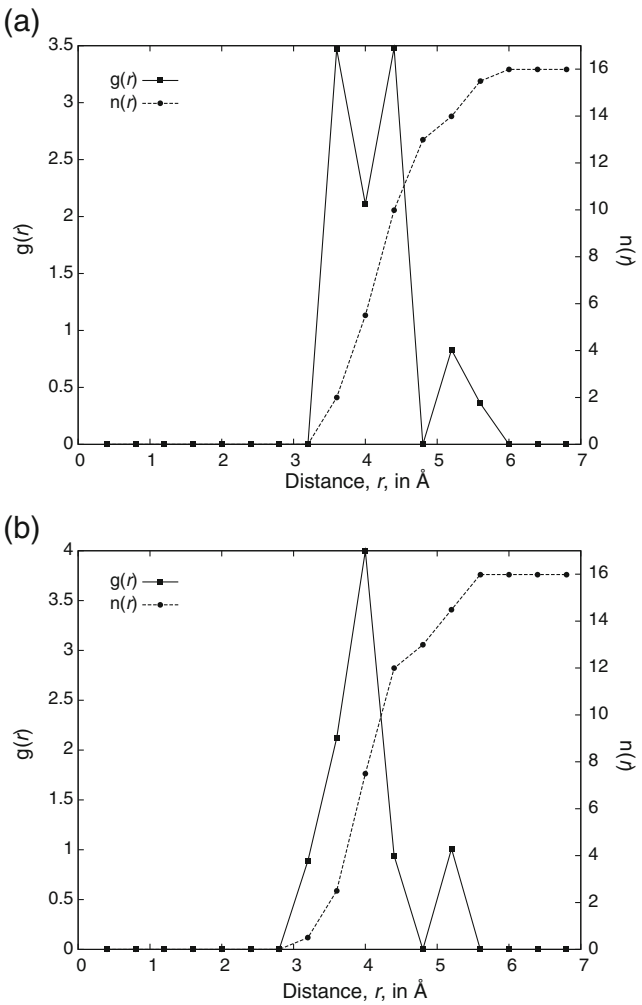

Fig. 5 Radial distribution function and running coordination number for $CaC_2O_4(H_2O)_{16}$ at **a** HF/6-31G* level of theory, and **b** RI-MP2/def2-SVP level of theory

the electrostatic attraction between the positively charged calcium and the partially negative oxygen atoms. Solvation reduces the C-O bond length, but not enough to equal the C-O bond lengths of the distal oxygens.

As expected, solvation somewhat pulls the calcium away from the oxalate, as seen in the Ca-C and the Ca-$O_{oxalate}$ distances in Table 2. The O-C-C angles also show asymmetry

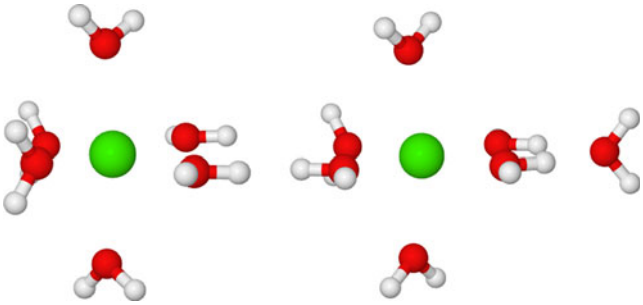

Fig. 6 Optimized geometries for $Ca^{2+}(H_2O)_6$ y $Ca^{2+}(H_2O)_7$ using RHF/6-31G* level of theory

similar to the C-O bonds: the angles closer to the calcium are more acute that the distal ones, but solvation does not seem to reduce the asymmetry as more water molecules are added.

From Table 2, the most remarkable results are the variations in the O-C-C-O dihedral angle in both oxalate ion and calcium oxalate. In anionic oxalate—starting from the gas phase result of 90°—solvation partially reduces the repulsion between the negative charges so the final dihedral angle is 78.3°. Calcium oxalate starts with a flat O-C-C-O angle (−0.1°) that reaches a maximum of 59.2° with 6 water molecules, and then slowly becomes flatter, reaching a minimum of approximately 15° with 14 water molecules to later get back to 50° with 16. The oxalate in unsolvated calcium oxalate is completely flat, but as solvation progresses, both carbons are slightly pyramidalized, as shown by the differing dihedrals reported in Table 2.

From Table 3, we observe that HF/6-31G* consistently yields shorter distances than MP2/6-311+G**. This is to be expected, due to the lack of dynamic electron correlation in HF, and the smaller basis set we used. The average unsigned error of HF vs MP2 is 2.61 %, while the error in HF compared to the only point with experimental validation is equal to or less than 4.05 %. The nice agreement between HF and MP2 when n=6 is most likely due to a fortuitous cancellation of errors.

The solvated oxalate anion shows an unsymmetrical distribution of the water molecules. When *n*=4, instead of a

Table 4 Number of hydrogen bonds for $C_2O_4^{2-}(H_2O)_n$ and $CaC_2O_4(H_2O)_n$

n	1	2	3	4	5	6	7	8	9	10	11	12[a]	13	14	16
$C_2O_4^{2-}(H_2O)_n$															
Number of oxalate-water H-bonds	2	4	6	7	8	9	9	10	11	12	11	12(12)	13	12	n.d.
Number of water-water H-bonds	0	0	0	0	2	3	5	6	7	8	10	11(12)	13	16	n.d.
$CaC_2O_4(H_2O)_n$															
Number of oxalate-water H-bonds	1	2	3	3	3	5	4	6	6	6	6	5	6	6	8
Number of water-water H-bonds	0	0	0	1	2	3	5	6	7	10	11	12	15	17	17

[a] Value in parenthesis from ref. [40], the more stable isomer

Table 5 Total hydration enthalpies ($\Delta_{hyd}H$) at the RHF/6-31G* level, in kcal mol^{-1} at 298.15 K, for $X + nH_2O \rightleftharpoons X(H_2O)_n$ when X = Ca(II), $C_2O_4^{-2}$ or CaC_2O_4

n	Ca(II)	$C_2O_4^{-2}$	CaC_2O_4
1	−53.13 (−55.0)[a]	−27.08	−28.59
2	−100.93 (−103.1)[a]	−51.80	−55.89
3	−143.44 (−146.2)[a]	−72.24	−78.72
4	−180.88 (−183.7)[a]	−91.49	−95.36
5	−210.47 (−213.8)[a]	−101.73	−111.67
6	−235.77 (−241.0)[a]	−116.58	−126.53
7	−254.14	−130.78	−139.29
8	−271.81	−143.56	−153.16
9	−286.23	−154.63	−160.99
10	−299.39	−165.95	−172.83
11	−309.86	−174.44	−183.51
12	−321.59	−183.25	−190.75
13	−332.51	−192.76	−198.88
14	−341.66	−199.83	−205.48
15	n.d.	n.d.	−214.70
16	n.d.	n.d.	−218.41

[a] from ref. [59]

C_4-symmetric distribution of the water molecules—H-bonded to the oxalate—one of the water molecules forms a H-bond to another water molecule (see Fig. 1). In the formation of the solvation shell of calcium oxalate, the governing factor is coordination of the water molecules. We observe a lopsided solvation shell (see Fig. 2), that we interpret as calcium more strongly coordinating the water molecules than the oxalate because of the highest charge density on calcium.

Figure 3, shows that the running coordination number has one clear plateau at six molecules of water, and there is another, less well defined, plateau between ten and 11 water molecules. According to $g(r)$, the first solvation shell is located up to 2.8 Å, while the second solvation shell reaches until 5.7 Å.

Figure 4 indicates that the first solvation shell of the oxalate ion is reaches out to 6.3 Å and includes 14 water molecules. According to Fig. 5, the first solvation shell of calcium oxalate contains 13 water molecules, and is located out to 6.0 Å of the geometric centroid of the calcium oxalate ion pair.

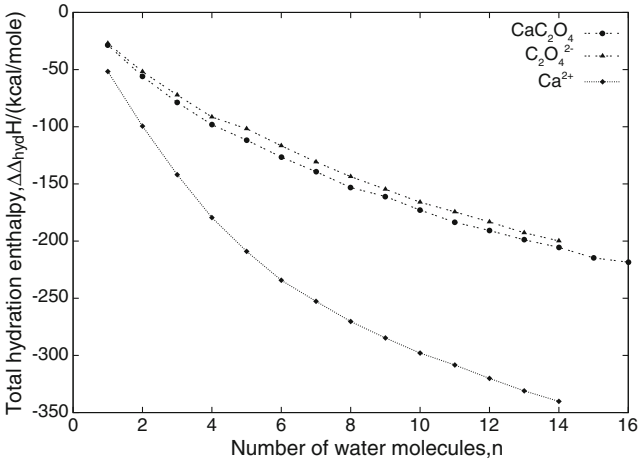

Fig. 7 Total hydration enthalpies, at 298.15 K, for calcium oxalate and its ions with *n* water molecules at the HF/6-31G* level of theory

The coordination number of hydrated Ca(II) is subject to considerable controversy, with reports covering all the range of (even non-integer) values from six to nine. Our RDF plots show that Ca(II) coordinates to six water molecules (Fig. 3), while the oxalate ion completes its first solvation shell with 14 molecules of water (Fig. 4), being directly H-bonded to 12 of them. Calcium oxalate completes its first solvation shell with 13 water molecules (Fig. 5). Calcium oxalate seems to hold fewer water molecules because of its neutral character, as opposed to the negatively charged oxalate ion. This should also have an effect on the hydration energies.

How do hydrogen bonds help stabilize the solvation shells? In Ca(II), hydrogen bonding starts only after the first solvation shell is complete (see Table 4 and Fig. 6). Figure 6 shows that the seventh water molecule is not directly coordinated to the calcium, so we can consider it part of the second solvation shell. In oxalate ion, the large negative charges promote H-bonding from the water molecules. Water-water H-bonding starts when there are five water molecules, and the inter-water H-bonds steadily increase up to 16, for the largest structure we examined ($C_2O_4^{2-}(H_2O)_{14}$). The number of oxalate-water H-bonds is always larger than the number of water-water H-bonds, except for the case with 14 water molecules. This might indicate the point where cooperativity among the water-water H-bonds yields a larger energetic advantage over oxalate-water H-bonding, in

Table 6 Best-fit parameters for hydration enthalpies in the equation $\Delta_{hyd}H^\circ = \frac{a}{(n+3)^2} + \frac{b}{n+3} + c$

	a	*b*	*c*	R^2	Standard error of *c*
Ca(II)	−3724.68	2648.57	−480.78	0.9998	2.31
$C_2O_4^{2-}$	−3941.09	2070.95	−302.79	0.9944	7.21
CaC_2O_4	−3814.57	2072.55	−312.73	0.9958	5.51

spite of the large negative charges on the oxalate oxygens. In calcium oxalate we observe a weaker tendency to form oxalate-water H-bonds, at least partly because the oxalate charge is neutralized by the positive charge on the calcium, however, the water-water H-bonds follow a pattern very similar to that in the oxalate anion.

Hydration energies

Our hydration energies for Ca(II) (see Table 5) approach the values calculated by Webb [59] with an absolute error of less than 3.4 %. For the other species, we lack values for comparison.

The data in Table 5 were fit to a function of form $\Delta_{hyd}H^{\circ} = \frac{a}{(n+3)^2} + \frac{b}{n+3} + c$, where n is the number of water molecules, and a, b, and c are empirical parameters resulting from the fit (see Table 6). The term $n+3$ was chosen because it yielded the smallest standard error for the c parameter of Ca(II). Graphically, c is the asymptote of the function on the ordinate axis, and we interpret it as the limiting value—at infinite dilution—of the hydration enthalpy (in kcal mol^{-1}, shown in Fig. 7). From the fit, when $n\rightarrow\infty$, the enthalpies of hydration approach −480.78 kcal mol^{-1} for Ca(II), −302.79 kcal mol^{-1} for the oxalate ion, and −312.73 kcal mol^{-1} for calcium oxalate. As the hydration energies approach an asymptotic limit, it is expected that their differential enthalpies will monotonically be less negative, as the number of water molecules increases. Table 7 agrees with this reasoning, showing that the differential gain upon addition of a water molecule is reduced with each new molecule added. It also shows that our results, despite not including dynamic correlation, are close to the experimental results. We attribute this better agreement to the configurational search performed on the solvation shells.

Table 7 Differential hydration enthalpies, $\Delta_{diff}H°$, (kcal mol^{-1}) for $X(H_2O)_{n-1} + H_2O \leftrightharpoons X(H_2O)_n$

n	Previous work on solvated Ca^{2+}			RHF/6-31G*[d]		
	MP2(FULL)/HUZSP*(p,d)[a]	Blackbody infrared radiative dissociation (BIRD)[b]	Ion-chamber[c] mass spectrometry	Ca^{2+}	$C_2O_4^{2-}$	CaC_2O_4
1	−56.1			−53.13	−27.08	−28.59
2	−51.6			−47.80	−24.71	−27.30
3	−47.9			−42.50	−20.44	−22.83
4	−42.7			−37.44	−19.26	−19.47
5	−34.2	−26.7		−29.59	−10.23	−13.48
6	−31.8	−22.0	−25.3	−25.30	−14.85	−14.86
7	−21.4	−16.8	−16.9	−18.38	−14.20	−12.76
8	−20.3		−16.1	−17.66	−12.78	−13.87
9	−13.7		−15.3	−14.42	−11.07	−7.83
10			−14.5	−13.16	−11.32	−11.84
11			−13.3	−10.46	−8.49	−10.69
12			−13.0	−11.73	−8.81	−7.23
13			−12.4	−10.92	−9.51	−8.14
14			−11.9	−9.16	−7.07	−6.59

[a] MP2(FULL)/HUZSP*(p,d)//RHF/HUZSP*(p) from ref. [14]

[b] B3LYP/LACVP** from ref. [17]

[c] Mass spectrometry ion chamber results from ref. [38]

[d] This work

Table 8 Stepwise water-binding electronic energies ($\Delta_{step}E$) at the RHF/6-31G* level, in kcal mol^{-1}, for $CaC_2O_4(H_2O)_n$, $C_2O_4^{2-}(H_2O)_n$ and $Ca^{2+}(H_2O)_n$ clusters, calculated according to the equation $\Delta_{step}E = E\ X(H_2O)_n - (E\ X(H_2O)_{n-1} + E\ H_2O)$

n	$Ca^{2+}(H_2O)_n$	$C_2O_4^{2-}(H_2O)_n$	$CaC_2O_4(H_2O)_n$
1	−53.94 (−56.90)[a]	−29.15	−30.43
2	−49.50 (−47.50)[a]	−26.78	−29.12
3	−44.20 (−42.00)[a]	−22.48	−24.56
4	−39.10 (−35.60)[a]	−21.19	−18.69
5	−31.29 (−27.70)[a]	−12.74	−18.54
6	−26.89 (−24.70)[a]	−16.98 (−15.7)[b]	−17.02
7	−20.54 (−13.80)[a]	−16.66 (−15.6)[b]	−15.06
8	−18.96 (−8.80)[a]	−14.89 (−15.3)[b]	−16.16
9	−17.50	−13.32 (−13.4)[b]	−9.95
10	−15.23	−13.32 (−12.7)[b]	−13.73
11	−12.12	−10.73 (−16.1)[b]	−13.25
12	−13.25	−10.99 (−13.2)[b]	−9.19
13	−13.40	−11.88	−9.56
14	−10.70	−9.15	−9.38
15	n.d.	n.d.	−11.23
16	n.d.	n.d.	−6.44

[a] Results at B3LYP/aug-cc- pVDZ//B3LYP/6-31+G** level from ref. [41]

[b] Results at B3LYP/6-311+G(2d,2p)//B3LYP/LANL2DZ level from ref. [35].

Table 8 and Fig. 8 shows the diminishing contribution to the binding electronic energy after the addition of another water molecule. Although at first sight the numbers may appear to vary monotonically, the variation is somewhat

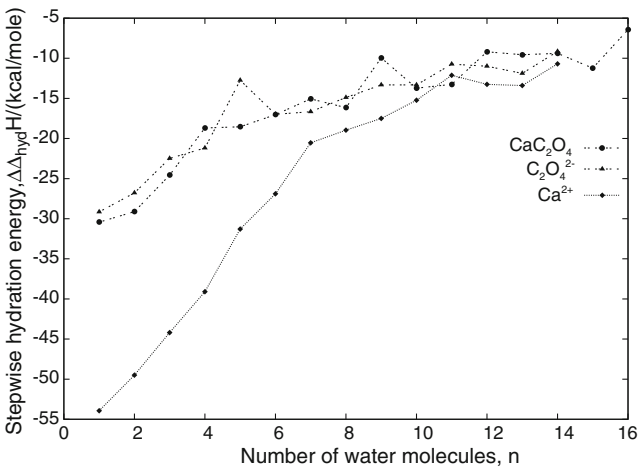

Fig. 8 Stepwise hydration energies, 298.15 K, for calcium oxalate and its ions with n water molecules at the HF/6-31G* level of theory

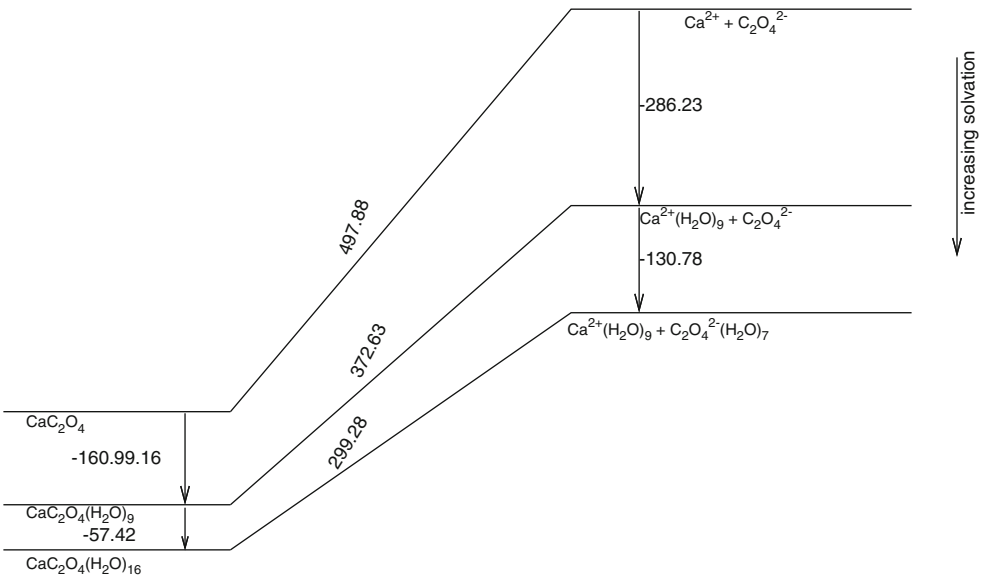

Fig. 9 Dissociation enthalpies for $CaC_2O_4(H_2O)_n \rightarrow Ca(H_2O)_m + C_2O_4^{2-}(H_2O)_{n-m}$ clusters, n=0-16, 298.15 K

irregular, probably due to the structural rearrangement required to minimize the energy after the addition of a water molecule. The variation resembles only qualitatively that of the differential enthalpies.

Figure 9 depicts the trends for the dissociacion of $CaC_2O_4(H_2O)_n$ complexes, as n increases. The energetic cost of separating the ions of CaC_2O_4 is 497.88 kcal mol^{-1}. When nine molecules of water are added the ions are stabilized by −372.63 kcal mol^{-1} but the CaC_2O_4 is stabilized by −160.99 kcal mol^{-1}. As we continue adding water molecules, when we reach 16, the energetic cost of separating the (now solvated) ions is still −299.28 kcal mol^{-1}. So it appears likely that energetic stabilization due to solvation of the ions is never large enough to make the solvated dissociated ions more stable than solvated CaC_2O_4. The asymptotic behavior determined from our fits is consistent with this: the largest enthalpy of hydration (−480.78 kcal mol^{-1} for Ca(II)) is still not enough to overcome the −497.88 kcal mol^{-1} energetic penalty incurred by the dissociation to the bare ions, so no amount of solvation can stabilize the ions to make them lower in energy than solvated CaC_2O_4, so, the dissociation reaction under solvation will be displaced toward the undissociated solvated calcium oxalate. This is consistent with the low Ksp that this salt presents, as the energetics justify the formation of a very small amount of solvated ions.

Table 9 Ca…M distance, in Å, for $CaC_2O_4(H_2O)_n$, (n=0 to 16). M is the centroid of the oxalate ion. O-C-C-O dihedral angle uses the oxygens closest to the Ca(II) and is expressed as absolute value

n	Distance/Å	O-C-C-O dihedral/°	n	Distance/Å	O-C-C-O dihedral/°
0	2.81	0.1	9	2.92	22.4
1	2.85	17.0	10	2.96	31.3
2	2.88	28.0	11	3.01	27.8
3	2.95	22.1	12	2.99	56.5
4	2.79	57.1	13	3.04	14.0
5	2.91	48.9	14	3.00	14.5
6	2.92	59.2	15	3.05	32.9
7	2.85	66.4	16	3.03	47.7
8	2.87	65.0			

The easier dissociation promoted by solvation leads us to examine the evolution of the average distance between the Ca(II) and the oxalate ion (actually, its geometric centroid, designated by M). By a simple reasoning, we could expect that—as water molecules were added—the greater charge screening due to solvation would weaken the electrostatic attraction and so the Ca…M distance would steadily increase. Table 9 shows the change in average distance between calcium and M as water molecules are added. The values start at 2.81 Å when n=0, and end at 3.05 Å when n=16, but instead of observing a monotonic increase in the distance, we observe a complex interplay between the O-C-C-O dihedral angle and the Ca…M distance. Reductions in Ca…M distance are always associated to a larger O-C-C-O dihedral angle (e.g., n=3→4, n=6→7 and n=15→16), although the converse is not true.

Conclusions

The determination of the global minimum geometry seems necessary to get reliable results. Ab initio RHF/6-31G* calculations on geometries obtained by semiempirical molecular dynamics allowed simulation of hydration of Ca(II) within 98 % of the known experimental values, e.g., our Ca-O average distance for $Ca^{2+}(H_2O)_6$, 2.58 Å, differs 4 % from the 2.48 Å previously obtained by X-ray diffraction. When

combined with a configurational search, the HF/6-31G* level of theory finds that the first solvation shells of Ca(II), $C_2O_4^{2-}$ and CaC_2O_4 are formed by 6, 14 and 13 water molecules, respectively. The second solvation shell of Ca(II) is made up by another five water molecules.

In calcium oxalate, as the number of water molecules grows toward the first solvation shell, the average Ca-oxalate distance increases concomitantly although not regularly, because the oxalate is able to redistribute its charge density through conformational flexibility.

Once the first solvation shell is formed, reaching the $Ca^{2+}(H_2O)_6$ cluster, the addition of water molecules toward the second hydration shell does not seem to affect the Ca-O distances in the first shell, while water-water H-bond formation is observed starting with seven water molecules.

H-bonding in the solvation shell of both oxalate and calcium oxalate is preferentially toward the negatively charged oxygens, and water-water H-bonding starts until n=5. Because of its partially neutralized negative charge, the oxalate in calcium oxalate forms fewer hydrogen bonds with water, compared with oxalate by itself.

The dissociation of $CaC_2O_4(H_2O)_n$ into solvated ions is always endothermic for n=1-16, which is consistent with the reported experimental heat of solution. The total standard solvation enthalpies approach asymptotic limits of −480.78 kcal mol^{-1} for Ca(II), −302.79 kcal mol^{-1} for oxalate ion and −312.73 kcal mol^{-1} for calcium oxalate.

Acknowledgments The authors wish to acknowledge funding from Universidad Autónoma de Nuevo León through the Programa de Apoyo a la Investigación Científica y Tecnológica (PAICyT) program (grants #CN067-09 and #CA1731-07), and from Facultad de Ciencias Químicas.

References

1. Hinton JF, Amis ES (1971) Solvation numbers of ions. Chem Rev 71:627–674
2. Ohtaki H, Radnai T (1993) Structure and dynamics of hydrated ions. Chem Rev 93:1157–1204
3. Babu CS, Lim C (1999) Theory of ionic hydration: insights from molecular dynamics simulations and experiment. J Phys Chem B 103:7958–7968
4. Pal SK, Zewail AH (2004) Dynamics of water in biological recognition. Chem Rev 104:2099–2124
5. Bagchi B (2005) Water dynamics in the hydration layer around proteins and micelles. Chem Rev 105:3197–3219
6. Ball P (2007) Water as an active constituent in cell biology. Chem Rev 108:74–108
7. Bakker HJ (2008) Structural dynamics of aqueous salt solutions. Chem Rev 108:1456–1473
8. Wesson JA, Ward MD (2007) Pathological biomineralization of kidney stones. Elements 3:415–421
9. Fulton JL, Heald SM, Badyal YS, Simonson JM JM (2003) Understanding the effects of concentration on the solvation structure of Ca^{2+} in Aqueous solution. I: the perspective on local structure from EXAFS and XANES. J Phys Chem A 107:4688–4696
10. Zavitsas AA (2005) Aqueous solutions of calcium ions: hydration numbers and the effect of temperature. J Phys Chem B 109:20636–20640
11. Bendich A, Zilberboim R (2008) Calcium: chemistry and biology. ACS Symp. Ser, USA
12. Frausto da Silva JJ, Williams RP (1991) The biological chemistry of the elements. Oxford University Press, Oxford
13. Clapham DE (1995) Calcium signaling. Cell 80:259–268
14. Katz AK, Glusker JP, Beebe SA, Bock CW (1996) Calcium ion coordination: a comparison with that of beryllium, magnesium, and zinc. J Am Chem Soc 118:5752–5763
15. Clapham DE (2007) Calcium signaling. Cell 131:1047–1058
16. Piquemal JP, Perera L, Cisneros GA, Ren P, Pedersen LG, Darden TA (2006) Towards accurate solvation dynamics of divalent cations in water using the polarizable amoeba force field: from energetics to structure. J Chem Phys 125:054511
17. Rodriguez-Cruz SE, Jockusch RA, Williams ER (1999) Hydration energies and structures of alkaline earth metal ions, $M^{2+}(H_2O)_n$, n=5−7, M=Mg, Ca, Sr, and Ba. J Am Chem Soc 121:8898–8906
18. Rais J, Okada T (2008) Quantized hydration energies of ions and structure of hydration shell from the experimental gas-phase data. J Phys Chem B 112:5393–5402
19. Bakó I, Hutter J, Pálinkás G (2002) Car–Parrinello molecular dynamics simulation of the hydrated calcium ion. J Chem Phys 117:9838
20. Todorova T, Hünenberger PH, Hutter J (2008) Car–Parrinello molecular dynamics simulations of $CaCl_2$ Aqueous solutions. J Chem Theory Comp 4:779–789
21. Jalilehvand F, Spångberg D, Lindqvist-Reis P, Hermansson K, Persson I, Sandström M (2001) Hydration of the calcium ion. An EXAFS, large-angle X-ray scattering, and molecular dynamics simulation study. J Am Chem Soc 123:431–441
22. Tongraar A, Liedl KR, Rode BM (1997) Solvation of Ca^{2+} in water studied by Born–Oppenheimer Ab Initio QM/MM dynamics. J Phys Chem A 101:6299–6309
23. Schwenk CF, Loeffler HH, Rode RM (2001) Molecular dynamics simulations of Ca^{2+} in Water: comparison of a classical simulation including three-body corrections and Born–Oppenheimer ab initio and density functional theory quantum mechanical/molecular mechanics simulations. J Chem Phys 115:10808
24. Kerisit S, Parker SC (2004) Free energy of adsorption of water and metal ions on the 101 h4 Calcite surface. J Am Chem Soc 126:10152–10161
25. Schwenk CF, Rode BM (2004) Ab initio QM/MM MD simulations of the hydrated Ca^{2+} Ion. Pure App Chem 76:37–47
26. Larentzos JP, Criscenti LJ (2008) A Molecular dynamics study of alkaline earth metal–chloride complexation in aqueous solution. J Phys Chem B 112:14243–14250
27. Li X, Tu Y, Tian H, Ågren H (2010) Computer simulations of aqua metal ions for accurate reproduction of hydration free energies and structures. J Chem Phys 132:104505
28. Hamm LM, Wallace AF, Dove PM (2010) Molecular dynamics of ion hydration in the presence of small carboxylated molecules and implications for calcification. J Phys Chem B 114:10488–10495
29. Megyes T, Grósz T, Radnai T, Bakó I, Pálinkás G (2004) Solvation of calcium ion in polar solvents: an X-ray diffraction and ab initio study. J Phys Chem A 108:7261–7271
30. Peschke M, Blades AT, Kebarle P (2000) Binding energies for doubly-charged ions M^{2+}=Mg^{2+}, Ca^{2+} and Zn^{2+} with the ligands L=H_2O, acetone and N-methylacetamide in complexes M for n=1 to 7 from gas phase equilibria determinations and theoretical calculations. J Am Chem Soc 122:10440–10449
31. Bush MF, Saykally RJ, Williams ER (2007) Hydration of the calcium dication: direct evidence for second shell formation from infrared spectroscopy. ChemPhysChem 8:2245–2253

32. Bush MF, Saykally RJ, Williams ER (2008) Infrared action spectra of $Ca^{2+}(H2O)_{11–69}$ exhibit spectral signatures for condensed-phase structures with increasing cluster size. J Am Chem Soc 130:15482–15489
33. Lei XL, Pan BC (2010) Structures, stability, vibration entropy and IR spectra of hydrated calcium ion clusters $[Ca(H_2O)_n]^{2+}$ (n=1–20, 27): a systematic investigation by density functional theory. J Phys Chem A 114:7595–7603
34. Tofteberg T, Öhrn A, Karlström G (2006) Combined quantum chemical statistical mechanical simulations of Mg^{2+}, Ca^{2+} and Sr^{2+} in water. Chem Phys Lett 429:436–439
35. Pavlov M, Siegbahn PEM, Sandstrom M (1998) Hydration of beryllium, magnesium, calcium, and zinc ions using density functional theory. J Phys Chem A 102:219–228
36. Floris FM, Persico M, Tani A, Tomasi J (1994) Hydration shell structure of the calcium ion from simulations with ab initio effective pair potentials. Chem Phys Lett 227:126–132
37. Probst MM, Radnai T, Heinzinger K, Bopp P, Rode BM (1985) Molecular dynamics and X-ray investigation of an aqueous calcium chloride solution. J Phys Chem 89:753–759
38. Peschke M, Blades AT, Kebarle P (1998) Hydration energies and entropies for Mg^{2+}, Ca^{2+}, Sr^{2+}, and Ba^{2+} from gas-phase ion–water molecule equilibria determinations. J Phys Chem A 102:9978–9985
39. Wang XB, Yang X, Nicholas JB, Wang LS (2001) Bulk-like features in the photoemission spectra of hydrated doubly charged anion clusters. Science 294:1322–1325
40. Wang XB, Yang X, Nicholas JB, Wang LS (2003) Photodetachment of hydrated oxalate dianions in the gas phase, C2O42 − (H2O)n (n=3–40): from solvated clusters to nanodroplet. J Chem Phys 119:3631–3640
41. Gao B, Liu ZF (2005) First principles study on the solvation and structure of $C_2O_4^{2-}(H_2O)_n$, n=6−12. J Phys Chem A 109:9104–9111
42. Marcus Y (2009) Effect of ions on the structure of water: structure making and breaking. Chem Rev 109:1346–1370
43. Thanthiriwatte KS, Hohenstein EG, Burns LA, Sherrill CD (2011) Assessment of the performance of DFT and DFT-D methods for describing distance dependence of hydrogen-bonded interactions. J Chem Theory Comput 7:88–96
44. Ireta J, Neugebauer J, Scheffler M (2004) On the accuracy of DFT for describing hydrogen bonds: dependence on the bond directionality. J Phys Chem A 108:5692–5698
45. Hassinen T, Peräkylä M (2001) New energy terms for reduced protein models implemented in an off-lattice force field. J Comp Chem 22:1229–1242
46. Stewart JJP (2008) MOPAC2009. Colorado springs, CO, USA: Stewart Computational Chemistry. http://OpenMOPAC.net
47. Schmidt MW, Baldridge KK, Boatz JA, Elbert ST, Gordon MS, Jensen JH, Koseki S et al (1993) General atomic and molecular electronic structure system. J Comp Chem 14:1347–1363
48. ORCA (2012) An ab initio, density functional and semiempirical program package, Version 2.9. University of Bonn
49. Martínez L, Andrade R, Birgin EG, Martínez JM (2009) PACKMOL: a package for building initial configurations for molecular dynamics simulations. J Comp Chem 30:2157–2164
50. Jmol a 3D molecular visualizer (2012) http://www.jmol.org Accessed 26 Jan 2011
51. Persistence of Vision Pty. Ltd. Persistence of Vision Raytracer (Version 3.6) http://www.povray.org
52. GNU Image Manipulation Program v.2.6.7. Cropping and color-to-grayscale transformation of the ray-traced images used GIMP v.2.6.7. http://www.gimp.org. Accessed 26 Jan 2011
53. Stewart JJP (2007) Optimization of parameters for semiempirical methods V: modification of NDDO approximations and application to 70 elements. J Mol Mod 13:1173–1213
54. Tanaka M, Aida M (2004) An ab initio mo study on orbital interaction and charge distribution in alkali metal aqueous solution: Li^+, Na^+, and K^+. J Sol Chem 33:887–901
55. Colonna-Cesari F, Sander C (1990) Excluded volume approximation to protein-solvent interaction. the solvent contact model. Biophys J 57:1103–1107
56. Ohio Supercomputer Center, Calculate Thermodynamics Properties from Gaussian Output. http://www.osc.edu/supercomputing/gridchem/UsersManual/ch09s04.html. Accessed 2 Dec 2010
57. Paniagua JC, Mota Valeri F (2010). Dipòsit Digital de la UB. (U. de Barcelona, Ed.) http://diposit.ub.edu/dspace/handle/2445/13382. Accessed 2 Dec 2010
58. Woon DE, Dunning TH (1995) The pronounced effect of microsolvation on diatomic alkali halides: ab initio modeling of MX $(H_2O)_n$ (M=Li, Na; X=F, Cl; n=1-3). J Am Chem Soc 117:1090–1097
59. Merrill GN, Webb SP, Bivin DB (2003) Formation of Alkali Metal/Alkaline earth cation water clusters, $M(H_2O)_{1–6}$, $M=Li^+$, Na^+, K^+, Mg^{2+}, and Ca^{2+}: An Effective Fragment Potential (EFP) Case Study. J Phys Chem A 107:386–396